ARTICLES
PUBLISHED ONLINE: 28 FEBRUARY 2010 | DOI: 10.1038/NPHOTON.2010.28
nature photonics

Real-time full-field arbitrary optical waveform measurement

Nicolas K. Fontaine*, Ryan P. Scott, Linjie Zhou, Francisco M. Soares, J. P. Heritage and S. J. B. Yoo

The development of a real-time optical waveform measurement technique with quantum-limited sensitivity, unlimited record lengths and an instantaneous bandwidth scalable to terahertz frequencies would be beneficial in the investigation of many ultrafast optical phenomena. Currently, full-field (amplitude and phase) optical measurements with a bandwidth greater than 100 GHz require repetitive signals to facilitate equivalent-time sampling methods or are single-shot in nature with limited time records. Here, we demonstrate a bandwidth- and time-record scalable measurement that performs parallel coherent detection on spectral slices of arbitrary optical waveforms in the 1.55 μm telecommunications band. External balanced photodetection and high-speed digitizers record the in-phase and quadrature-phase components of each demodulated spectral slice, and digital signal processing reconstructs the signal waveform. The approach is passive, extendable to other regions of the optical spectrum, and can be implemented as a single silicon photonic integrated circuit.

The ability to accurately characterize ultrafast optical waveforms affects nearly all fields of science and technology. For example, in optical arbitrary waveform generation (OAWG)[1–4], an optical bandwidth of hundreds of gigahertz as well as gigahertz update rates have been achieved, and optical communications technologies are spanning terahertz bandwidths by making use of advanced amplitude/phase modulation formats[5–7]. Applications such as solid-state quantum information processing[8] and the investigation of many transient optical phenomena[9,10] require optical waveform measurements on the sub-picosecond timescale. In many of these disciplines it is not sufficient to quantify only the temporally varying optical intensity; instead, the full-field optical waveforms must be measured over long record lengths in a single shot. Our interest therefore lies solely in techniques that fully characterize the amplitude and phase of non-repetitive optical waveforms.

Frequency-resolved optical gating (FROG)[11] and other nonlinear optical techniques[12] make use of both the time and frequency domains to measure the amplitude and phase of optical waveforms with sub-femtosecond resolution. Single-shot implementations of these techniques generally require significant pulse energies[11,13,14], and any technique that relies on large two-dimensional detector arrays has a limited update rate[15–17]. A different technique, heterodyne temporal imaging[18,19], uses the space–time analogy to temporally magnify ultrafast optical waveforms and heterodyne beating with a single frequency reference to estimate the signal phase. Recent demonstrations show a resolution of 100 fs (refs 18,19), but the record lengths are limited to hundreds of picoseconds by the pump pulse duration. Spectral interferometry (SI)[20–22] measurement techniques, including single-shot variants[15,16,23,24], achieve excellent sensitivity because they take advantage of coherent detection gain but do not resort to optical nonlinearities. However, spectral resolution requirements restrict record lengths to less than a few nanoseconds[25,26], and because of this limitation they are impractical to scale to continuous time recording. It is commonly asserted that the effective time record for many of the single-shot techniques can be increased by using some type of time interleaving[27,28]. However, time-interleaved demonstrations of single-shot, full-field waveform measurements have not been reported in the literature to date. This is not surprising, because it is difficult to parallelize or integrate measurement schemes that rely on combining and synchronizing multiple time gates.

Recently, the availability of gigahertz-bandwidth digitizers has renewed interest in optical digital coherent receivers[6,7,29] for fibre communications because it has become possible to track the carrier phase without the use of phase-locked loops[29]. The digital coherent receiver measures the full optical field by digitizing the photodetected in-phase (I) and quadrature-phase (Q) signals from a phase-diversity (multiport) homodyne receiver[30,31], and then reconstructs the optical waveform using digital signal processing (DSP)[32,33]. When quadrature sampling bandpass signals, the Nyquist-limited I/Q sampling rate is half the standard real-signal sampling rate[34]. Therefore, the optical measurement bandwidth is twice the electrical bandwidth of the digitizer, which is currently limited to a few tens of gigahertz. The method described in this Article uses an optical digital coherent receiver and, at the same time, enables a scalable optical bandwidth without increasing the electrical bandwidth to perform real-time, full-field optical waveform measurements. We demonstrate an instantaneous bandwidth of greater than 160 GHz with record lengths of 2 μs, which represents the largest record length-to-resolution ratio (>320,000) of any single-shot, full-field measurement technique.

Concept and implementation

Figure 1 shows an illustration of a technique we refer to as real-time 'optical arbitrary waveform measurement' (OAWM). It combines spectral slicing of the optical signal with parallel optical homodyne detection using an optical frequency comb (OFC) as a reference. Spectral slicing is conceptually similar to the bandwidth interleaving or frequency interleaving[35–37] techniques used in some high-speed digitizers. Figure 1 (top) shows a time-varying signal waveform with a particular optical bandwidth and, on the left side of the figure, a stable reference OFC spanning the spectrum of the signal. A gapless spectral demultiplexer (that is, partially overlapping adjacent passbands) directs 'slices' of the incoming signal spectrum to separate spatial locations (for example, separate waveguides). Simultaneously, a different narrow passband spectral

Department of Electrical and Computer Engineering, University of California, Davis, One Shields Ave., Davis, California 95616, USA.
*e-mail: nkfontaine@ucdavis.edu

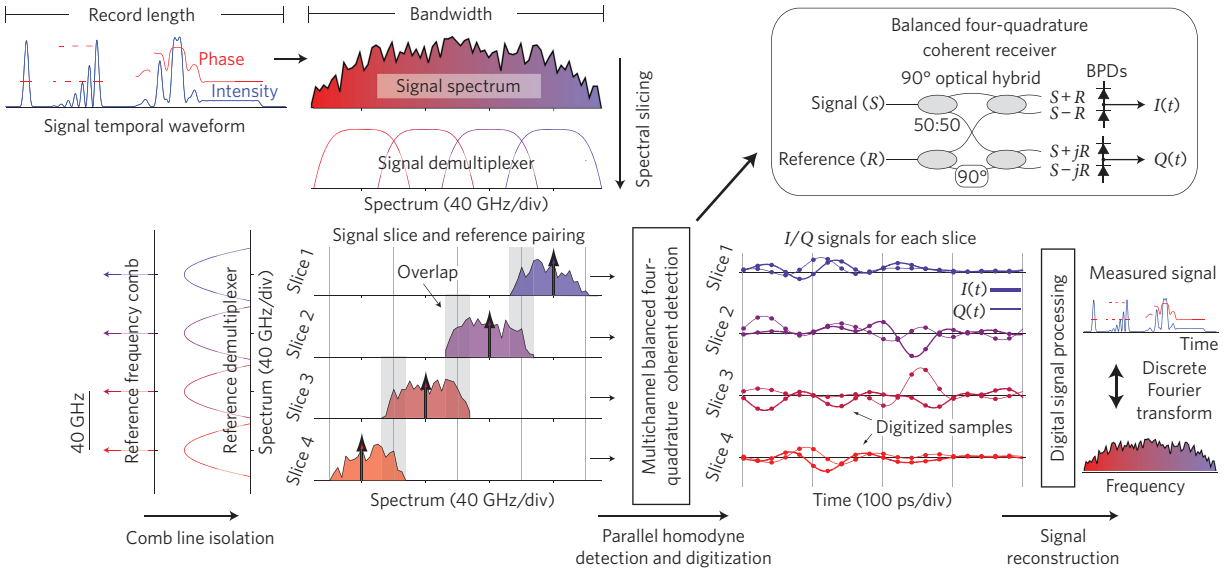

Figure 1 | Illustration of the real-time OAWM technique. The signal spectrum is sliced by a gapless spectral demultiplexer, and each line of a reference frequency comb is isolated by a second spectral demultiplexer. In a parallel operation, the optical signal from each slice is demodulated to the baseband using balanced four-quadrature coherent detection. Sampling the in-phase (I) and quadrature-phase (Q) signals above the Nyquist rate for quadrature signals (50 GS s^{-1} indicated) captures the full slice bandwidth (40 GHz). The inset details how a 90° optical hybrid and balanced photodiodes (BPDs) generate I/Q signals for a single spectral slice (j is the imaginary unit).

demultiplexer strongly isolates each line of the reference OFC. Then, in a parallel manner, each spectral slice is coherently demodulated by a single comb line to baseband temporal I/Q signals using a separate four-quadrature coherent balanced receiver[31]. Digitizers synchronized to the reference frequency comb sample the baseband I/Q signals of the slices, and DSP superposes the signals to reconstruct the measured signal waveform. Naturally, accurate reconstruction requires knowledge of the transmission function of the signal multiplexer, the electronic responses of the photodiodes and digitizers, and the reference OFC amplitude and phase (obtainable by various multishot characterization techniques or even through self-calibration).

OAWM is a passive and free-running technique, because optical filtering, power splitting and combining are linear operations (for example, couplers, arrayed-waveguide gratings). Time-demultiplexing techniques, however, require a nonlinear effect (such as the Kerr or electro-optic effects) and a control signal to isolate temporal regions[38]. The coherent optical demodulation used by OAWM (inset of Fig. 1) demonstrates excellent sensitivity; it is also simple to implement over a broad bandwidth and includes coherent gain. Passive optical waveguides combine an optical reference carrier in four quadrature phases with a signal waveform. Mixing using square-law detection in a photodetector down-converts the signal waveform to baseband I/Q signals with bandwidths equal to the detection bandwidth. In OAWM, it is the digitization of the spectral slice I/Q signals that enables reconstruction of infinite-length time records (limited by available memory), although the parallel nature of OAWM provides scalability to infinite-bandwidth signals (limited only by the available component technology).

Additionally, in many measurement situations the spectrum of the signal waveform spans multiple spectral slices. The optical overlaps of adjacent slices (highlighted by grey bars in Fig. 1) are then useful for self-measurement of the reference comb and self-calibration, because there are two separate measurements of the overlapping spectra. The difference in measurement yields the amplitude and phase difference for adjacent reference comb lines.

Figure 2 shows the continuous OAWM experimental arrangement, demonstrating 160 GHz of instantaneous bandwidth for 2 μs. The top left half contains the signal waveform generation section and the right half shows the waveform measurement section. A combination of strong phase and amplitude modulation of a tunable single-frequency laser[39,40] centred at 1,550 nm generates the stable four line × 40 GHz reference OFC. The signal generation section creates complex and predictable waveforms having both wide bandwidths and slowly varying temporal features by alternating between two different wide-bandwidth waveforms[4] in various low-repetition-rate patterns. Both waveforms originate from a separate 10 GHz OFC, which uses an independent single-frequency laser, offset by ~200 MHz from the reference OFC. This purposely introduces random temporal phase fluctuations between the reference and the signal to demonstrate that it is unnecessary for them to be optically phase-coherent. Waveform A is a 160-GHz-wide, transform-limited, sinc^2-like pulse (that is, a flat spectral envelope with flat spectral phase) directly from the 10 GHz OFC. Waveform B is a 160-GHz-wide pulse with a Gaussian spectral envelope and cubic spectral phase crafted by static OAWG (that is, line-by-line pulse shaping)[2,41] with a 10 GHz silica planar lightwave circuit (PLC) based waveform shaper[42]. A 2 × 2 Mach–Zehnder modulator (that is, fast switch), driven by an electronic arbitrary waveform generator (EAWG) at 20 GS s^{-1} (9.6 GHz analogue bandwidth), alternates its output between waveform A and waveform B in a programmed sequence (for example, ABAABBAAA...).

The OAWM experiment uses a specially designed silica PLC, which integrates all the passive optical components necessary to implement spectral slicing and four-quadrature coherent detection. Balanced detection (that is, homodyne down-conversion) and digitizing occurs off-chip using d.c.-coupled 40 GHz balanced photodetectors connected to the inputs of eight 50 GS s^{-1} digitizers from two, four-channel real-time oscilloscopes. The OAWM PLC incorporates two arrayed-waveguide grating (AWG) spectral demultiplexers, both aligned to the reference OFC, with 16 output channels spaced at 40 GHz and an array of sixteen 90° optical hybrids. Single-mode fibre arrays couple signals in and out of the

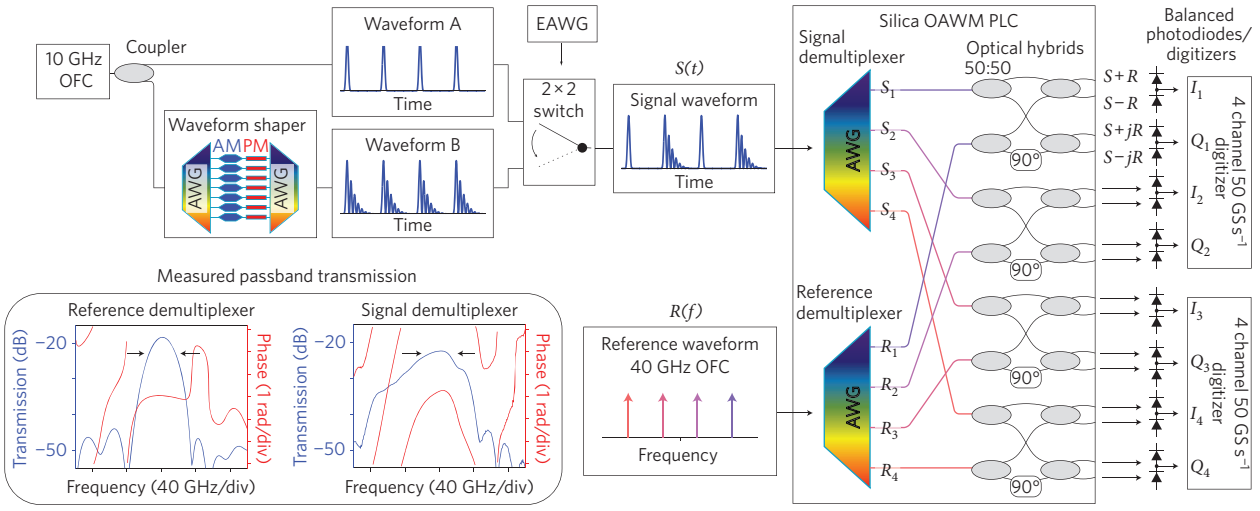

Figure 2 | Details of the arrangement used to demonstrate OAWM. Various signal waveforms are created by time-interleaving waveform A and waveform B using a 2 × 2 Mach–Zehnder modulator (switch) driven by an electrical arbitrary waveform generator (EAWG). The silica planar lightwave circuit (PLC) and balanced photodiodes provide in-phase/quadrature-phase (I/Q) signals for each spectral slice by means of balanced four-quadrature homodyne detection. A separate 40 GHz optical frequency comb (OFC) provides the reference waveform. The inset shows the measured transmission for a single channel from each of the two demultiplexers (arrows indicate 40 GHz). The digitizer clocks and the EAWG are synchronized to the 40 GHz OFC.

PLC. The signal AWG slices the signal $S(t)$ into slightly overlapping spectral slices (that is, S_1, S_2 and so on) and directs each slice to a different optical hybrid. The reference AWG demultiplexes and directs each comb line (that is, R_1, R_2 and so on) to the reference input of the corresponding optical hybrid. Then, each hybrid combines a spectral slice in four quadrature phases with a single reference comb line mathematically represented as $I_+ = S + R$ for 0°, $I_- = S - R$ for 180°, $Q_+ = S + jR$ for 90°, and $Q_- = S - jR$ for 270°. Four I_+/I_- and Q_+/Q_- pairs are coupled off chip to balanced photodiode pairs, which generate the I and Q signals. The eight signals are then digitized at 50 GS s^{-1} with 8 bits of resolution (that is, 256 levels).

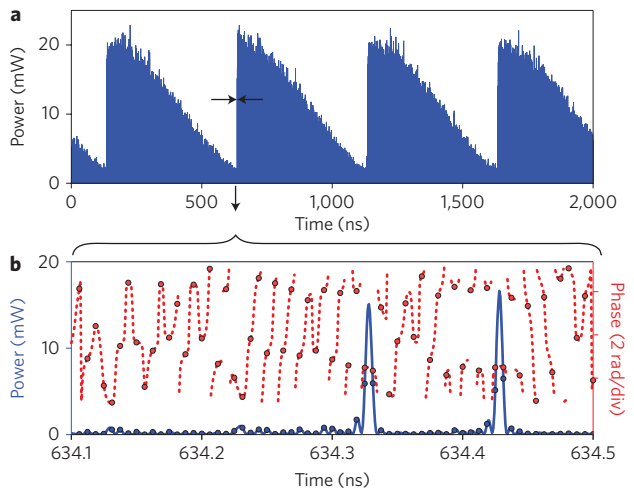

Figure 3 | Example OAWM measurement of a train of transform-limited pulses (waveform A) with an overall sawtooth amplitude envelope (0.5-μs period). a, Reconstructed signal waveform showing the complete 2-μs record length (phase information not shown for clarity). **b**, Window (400 ps) from **a** showing the detailed intensity and phase. Circles indicate the Nyquist-limited sampling rate (160 GS s^{-1} for the I and Q components (320 GS s^{-1} aggregate), 6.25 ps sample period) and the lines show the Fourier interpolation obtained by padding the data with zeros (1:8) in the frequency domain.

Each AWG fulfils a distinct function, one as a high-isolation demultiplexer for the reference OFC and the other as a gapless demultiplexer for signal slicing. The plot in the lower left corner of Fig. 2 shows that the reference AWG passbands have a −3 dB bandwidth of 25 GHz and better than −30 dB adjacent channel crosstalk, providing excellent reference comb line isolation. In contrast, the broader passbands of the signal AWG (40 GHz), and correspondingly larger adjacent channel crosstalk (−15 dB), slice the signal spectrum without excess filtering at the edges of the slice.

Measurement examples

Several distinct waveform measurement examples demonstrate the various aspects and unique capabilities of OAWM. The first example involves a waveform that illustrates measurements with high temporal resolution over long record lengths. Second, we show a measurement of a repetitive waveform B, the cubic spectral phase waveform. The repetitive nature of the waveform enables comparison with well-established multishot measurement techniques (for example, FROG) and it eases interpretation of the spectrum. Finally, we show a complex, low-repetition-rate waveform that contains both waveform A and waveform B in a programmed fashion. For the figures in this section, the time-domain plots display the instantaneous optical signal power and the spectral plots show the average optical signal power per spectral bin (500 kHz) at the photodiodes.

Figure 3a shows the temporal intensity of a long waveform composed of waveform A, a sinc^2-like waveform repeating every 100 ps, modulated with a relatively slowly varying sawtooth intensity envelope. The envelope is created by driving the 2 × 2 Mach–Zehnder modulator with a voltage ramp from the EAWG that is switched on in less than 100 ps and then slowly switched off over 500 ns. Figure 3b shows the intensity and phase of the waveform for a 400-ps window of the time record at a fast rising transition of the ramp. Within the window, waveform A abruptly switches on and it has sub-pulses with phase alternating between 0 and π rad (that is, alternating between negative and positive fields). The 6.25-ps sampling interval determines the minimum resolvable temporal feature, as is made evident by the two samples within the ∼6-ps-wide pulse peak.

Figure 4a shows a 400-ps window from a 2-μs-long measurement of a 100-ps periodic train of pulses that consists solely of

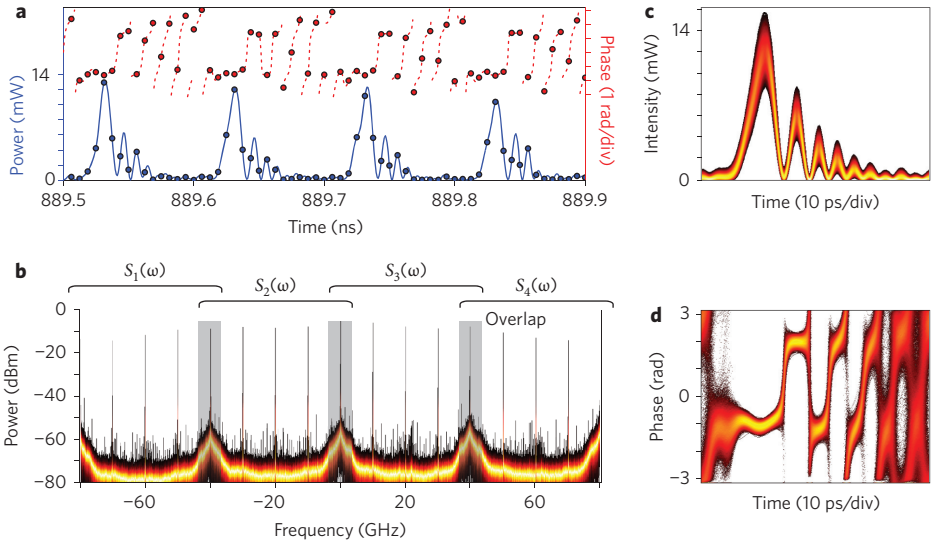

Figure 4 | OAWM measurement of a 10 GHz train of pulses with cubic spectral phase (waveform B). a, Window (400 ps) from a 2-μs temporal record. **b**, Spectra of the four measured slices centred at ~1,550 nm, 62.5 MHz displayed resolution (2 μs temporal record). **c**, Histogram built from 100-ps windows taken from the full temporal record, showing the statistics of the pulse-to-pulse fluctuations in intensity. **d**, Corresponding phase histogram across the full time record, with the linear temporal phase removed.

waveform B. The distinctive asymmetric ringing is indicative of the cubic spectral phase. With the full waveform information (intensity and phase), discrete Fourier transforms (DFT) allow either the time-domain and/or spectral-domain representations to be displayed. Figure 4b shows the spectral intensity of the four measured slices, indicating their relative positions and overlap. The colour gradient of the plot shows the minimum, maximum (black) and mean (yellow) power within each 62.5 MHz spectral bin (the measurement resolution is 500 kHz, which is the inverse of the time record). The strong 100-ps periodicity of waveform B creates the well-defined spectral lines. The overlap between the slices can either validate or measure the amplitude and phase values of the reference OFC. As an example, in each two centre slices, five spectral lines are measured, but one line is common to the two adjacent spectral slices. If the measured amplitude and phase of the common spectral lines are the same, then the calibrations are presumably correct. Figure 4c,d shows two-dimensional histograms (similar to eye diagrams) of the intensity and phase of waveform B obtained by overlaying each consecutive 100-ps window into one 100-ps frame. Histograms aid in visualizing the fidelity of the measurement by simultaneously showing many measurements of identical waveforms. The variations of the intensity histogram are larger at high intensity because the measurement noise adds linearly with the electric field rather than the intensity. For the phase histogram, the offset in reference and signal centre frequencies (~200 MHz) creates a linear temporal phase that has been removed (see Supplementary Information for further details). The sharp phase and intensity histograms indicate that the measurement fidelity is consistent across the 2-μs record.

Figure 5 compares a cross-correlation FROG (XFROG) measurement[11] of waveform B to the calculated OAWM average for the entire 2-μs time record (that is, 20,000 waveform Bs). The comb spectrum in Fig. 4b enables simple averaging across the whole time record by just selecting the intensity and phase of each spectral line. The close match between OAWM and FROG measurements indicates successful implementation and calibration of OAWM.

Figure 6a shows a measurement of a complex 4-ns repetitive waveform consisting of the following sequence of waveforms A and B: [ABAABBAAABBBAAAABBBBAAAAABBBBBAAAAABBBBB]. The pattern repeats 500 times in the 2-μs temporal record, forming a data set that is impractical to display within a standard-sized static figure. Instead, intensity histograms show the results for the full temporal record. To better understand the complex waveform and to highlight some of the measurement results, Fig. 6b shows a 600-ps window that contains the transition between waveform A as it is switched on and waveform B as it is switched off. Figure 6c,d shows the same transition with either waveform B blocked (Fig. 6c) or waveform A blocked (Fig. 6d). The switch maximizes the extinction of waveform B between its on and off states rather than waveform A. In Fig. 6b, waveform A transitions off as waveform B transitions on. Coherent interference effects between waveform A and waveform B can be seen when the intensities of the two waveforms are comparable, particularly at the first entrance of waveform B, where the two waveforms partially overlap. For further comparison, Fig. 6c shows only waveform A by blocking waveform B, and Fig. 6d shows only waveform B.

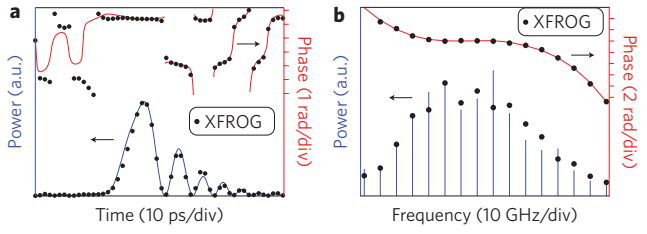

Figure 5 | Comparison to a well-established measurement technique. Comparison between averaged OAWM (solid lines) and an XFROG (dots) measurement of a repetitive cubic spectral phase waveform (FROG error, $G < 0.005$ for a 128×128 array). **a**, Comparison in the temporal domain. **b**, Match shown as spectral intensity and phase.

Discussion

The results demonstrate single-shot, full-field optical waveform measurements with an instantaneous bandwidth of 160 GHz. Most measurements use ~3 mW of reference power and ~500 μW of signal power for each slice, corresponding to an average of 12.5 fJ per sample point or per spectral bin. In OAWM, the measurement bandwidth is equal to the number of slices multiplied by the slice bandwidth. Thus, for a given measurement

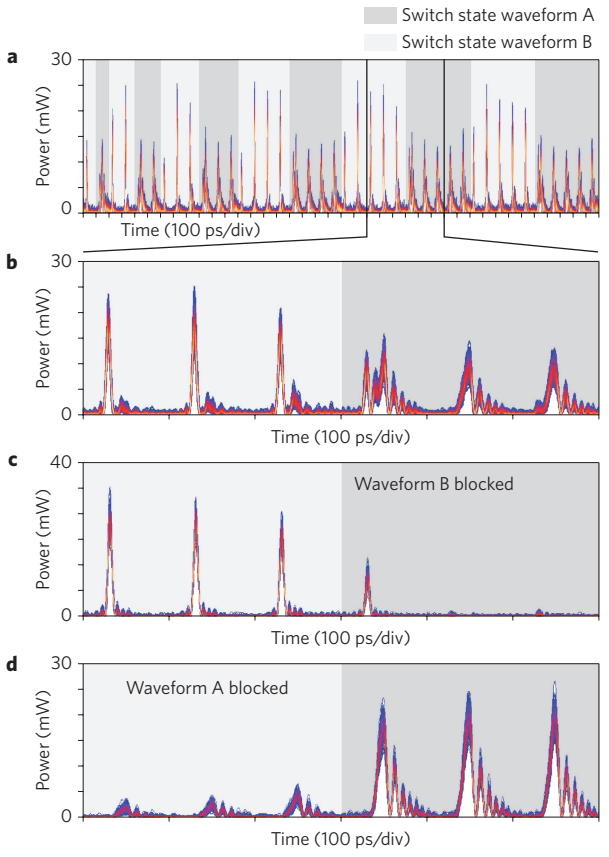

Figure 6 | OAWM measurement data for a complicated waveform pattern. **a**, Reconstructed signal waveform showing a histogram of the waveform intensity for the 4-ns pattern created from 2 μs of total data (phase information not shown for clarity). **b**, Window (600 ps) from **a** showing the detailed intensity histogram at one of the A-to-B transitions. **c**, Intensity histogram when waveform B is blocked. **d**, Intensity histogram when waveform A is blocked.

bandwidth, there is a trade-off between the number of spectral slices (more complex optics for more slices) and the slice bandwidth (more complex electronics for higher slice bandwidth) that must be optimized. The choice of a slice spacing of 40 GHz was dictated by the frequency range in which optical demultiplexers, photoreceivers and electronic digitizers overlap, while simultaneously maximizing the measurement bandwidth and minimizing system complexity. For instance, the fastest electronic digitizers have an analogue bandwidth of ~20–25 GHz and set an upper limit on the slice spacing. Higher-resolution AWGs require larger areas and set the lower limit of the slice spacing. In the silica PLC design, it was simple to put two 40 GHz AWGs and 16 optical hybrids on the same PLC (total OAWM bandwidth of 640 GHz); however it is more difficult to fit two AWGS with a resolution of 20 GHz within a standard-area PLC.

OAWM can potentially achieve quantum-limited sensitivity (that is, sensitive only to the fluctuations of the signal), because it uses a strong reference OFC to boost the detected signal level above the electronic noise level and balanced detection to suppress the common signal and reference intensity terms[43,44]. Like all coherent and interferometric techniques, OAWM measures the signal waveform with respect to a reference, and any reference OFC noise or systematic drift will transfer to the measurement. For example, centre frequency fluctuations of the reference OFC create a varying temporal phase error in the measurement, and the minimum measurable spectral feature is equal to the reference OFC linewidth (see Supplementary Information for further details). If present, fluctuations in the reference comb spacing will change the slice locations, which skews the measured spectrum. Fortunately, gigahertz-rate OFC generators have remarkable long-term and short-term stability[45], especially when frequency-stabilized to an absolute (atomic) reference. Here, the measurement fidelity is limited by the effective number of bits (ENOB) and rapid frequency roll off above 16 GHz of the digitizer rather than the reference OFC. ENOB is the measure of the effective accuracy of the digitizer, including effects from sampling jitter, signal distortion, quantization and noise. In these measurements, the digitized signal spans 3 bits of the available 4.4 ENOB for a digitizer-limited signal-to-noise ratio (SNR) of 20 dB. Also, after post-emphasis, 75% of the noise occurs above 16 GHz. Reducing excess optical losses and continued performance improvements in low-noise, high-speed digitizers will significantly increase the sensitivity.

There is a trade-off between measurement fidelity and slice bandwidth. Reducing the slice bandwidth permits higher-fidelity measurements, because slower digitizers with large ENOBs are available. For instance, a slice bandwidth of 2 GHz allows use of 2 GS s^{-1} digitizers, which are available with ~10 ENOB. However, this solution requires larger, higher-resolution AWGs and a greater number of slices and components to achieve a particular measurement bandwidth. The specific application of OAWM will ultimately dictate how to balance these engineering trade-offs.

The OAWM silica PLC is 16 × 40 GHz and, thus, will support 640 GHz measurements by using additional photodetectors and digitizers. Scaling the measurement bandwidth beyond 1 THz (sub-picosecond resolution) is practically challenging, especially with discrete components. However, integrating the optics, photodetectors, digitizers and electronic processing in monolithic or hybrid chips would significantly reduce system integration complexity and cost. A possible integration platform is silicon photonics[46,47], with recent reports of monolithic coherent receivers[48], high-resolution AWGs[49], and the integration of digitizers and DSP on a single application-specific integrated circuit (ASIC)[50].

A significant insight into the field of optical arbitrary waveform generation and measurement is possible once one realizes that OAWG is completely analogous to OAWM. As Fig. 1 shows, OAWM coherently demodulates slices of the spectrum of an optical signal and provides the temporal I/Q signals for each slice. After removing the effects of optical and electrical filters in the measurement system (AWG passbands, photoreceiver response and so on), the signal waveform is reconstructed from the slice I/Q signals using DSP. OAWG is the inverse of this process. Starting with an OFC, a spectral demultiplexer isolates each comb line to a separate waveguide. Then I/Q modulations, determined with DSP pre-processing, are applied separately to each OFC comb line. The spectrally broadened comb lines are combined using a multiplexer with spectrally overlapping adjacent passbands, producing the arbitrary optical waveform. The I/Q modulation signals must account for the optical filtering of the slice multiplexer and electrical response of the modulator and driving circuit. The spectrum of the resulting waveform is continuous, with the phase and amplitude fully specified across the entire bandwidth. If the modulation is continuously applied, the temporal length of the waveform can be infinite (just as the OAWM record length is theoretically infinite). Thus, OAWM is a corroboration of continuous and dynamic OAWG techniques.

Methods

Real-time versus equivalent-time sampling. The measurements capture 160 GHz of optical bandwidth in a single shot. This is a real-time, as opposed to an equivalent-time, technique, because the single-shot measurement bandwidth is the same as the instantaneous bandwidth (just as in sampling oscilloscope definitions[37]). Real-time sampling does not imply zero latency; in fact, processing and display of the 2 μs temporal record took ~50 ms on a 2.66 GHz Intel W3520 processor.

Optical frequency comb generator. Both OAWG and OAWM require a stable OFC. The ability to control the centre wavelength and the spacing of the frequency comb are necessary for alignment with the spectral demultiplexers. Each OFC generator strongly modulates a different tunable single-frequency laser using a separate dual-electrode Mach–Zehnder modulator (DEMZM)[40] (we used an Agilent 81642B for the 10 GHz signal OFC and a New Focus TLM-8700-L-CL for the 40 GHz reference OFC; both have <100 kHz optical linewidth). By controlling the two radio-frequency drive powers of the DEMZM, and their relative phases, both amplitude and phase modulation can be applied to the continuous-wave (c.w.) laser. The amplitude modulation carves a pulse train on the c.w. laser with a 50% duty cycle, and the phase modulation produces a broadened spectrum and a near-linear frequency chirp. The residual negative chirp of the OFC output is compensated by using positive dispersion in 1 km of single-mode fibre. The 10 and 40 GHz microwave signals that drive their respective DEMZMs are derived from a common 20 GHz oscillator. Radio-frequency synchronization of the 10 and 40 GHz OFCs is convenient for measurement analysis (for example, building histograms), but it is unnecessary for signal measurement.

Slice measurement and calibration. From Fig. 1, the four signals exiting the hybrid for a particular spectral slice are $I_+(t) = s_{I+}S(t) + r_{I+}R(t)$, $I_-(t) = s_{I-}S(t) - r_{I-}R(t)$, $Q_+(t) = s_{Q+}S(t) + jr_{Q+}R(t)$ and $Q_-(t) = s_{Q-}S(t) - jr_{Q-}R(t)$, where s and r represent the complex transmission of the signal and reference through the hybrid. Adjusting phase shifters inside each hybrid provides the proper phase shifts to the four coefficients. After photodetection on a single photodiode, the I signals are $|I_\pm(t)|^2 = |r_{I\pm}|^2\,|R(t)|^2 + |s_{I\pm}|^2\,|S(t)|^2 \pm 2s_{I\pm}\,r_{I\pm}\,\mathrm{Re}\{S(t)\,R^*(t)\}$. The difference signal from the balanced photodiodes provides either the I or Q component, which, after digitization, is $I(t) = |I_+(t)|^2 - |I_-(t)|^2 = (|r_{I+}|^2 - |r_{I-}|^2)\,|R(t)|^2 + (|s_{I+}|^2 - |s_{I-}|^2)\,|s(t)|^2 + 2(s_{I+}\,r_{I+} + s_{I-}\,r_{I-})\,\mathrm{Re}\{S(t)\,R^*(t)\}$ (ref. 15). This equation has two common terms proportional to the intensity of S and R and the mixing term proportional to the real part of S with respect to R. To remove the common terms, the signal path is first balanced by making s_{I+} equal to s_{I-} by using on-chip equalizers and then the common term proportional to R is removed by measuring R (a constant) and then subtracting it in subsequent measurements. The same procedure is followed for the digitized $Q(t)$ signal. These digitized signals are then Fourier-transformed to the frequency domain and processed as follows to obtain the full optical field of that spectral slice. The field in the ith slice is $S_i(f - f_i) = H_i(f) \times [E_{iI}(f)\,I(f) + jE_{iQ}(f)\,Q(f)]/R_i^*$ where f_i is the frequency of the ith reference comb line, $H_i(f)$ is the inverse signal spectrum filter, $E_{iI}(f)$ and $E_{iQ}(f)$ are the inverse electrical filters for $I(f)$ and $Q(f)$ components, and R_i is the phase and amplitude of the ith reference comb line. Combining the slices in the frequency domain produces the final waveform.

Measurement noise. In Fig. 4b, the 15 dB SNR is calculated by dividing the total power in the spectral lines by the integrated noise power. The power of each spectral line is ~60 dB above the slice centre noise floor (−70 dBm) and ~35 dB above the slice edge noise floor (−55 dBm). Post-emphasis for the fast roll-off of the digitizer's electrical response above 16 GHz and some spectral filtering from the signal AWG increases the noise floor. This shows a sensitivity of up to −70 dBm per spectral line for a 2 μs averaging period. Increasing the measurement window time would continue to lower the spectral noise floor, limited only by the quantization noise floor of the digitizer.

Oscilloscope trigger jitter. In the experiment, two oscilloscopes (Tektronix, DPO72004), each with four 50 GS s^{-1}, 8-bit digitizers, sample the d.c.-coupled I/Q signals directly from the balanced photodiodes (u^2t, BPDV2050RVF). To start each 2-μs acquisition, the oscilloscopes are triggered simultaneously from a common electrical pulse (rise time of ~100 ps) at a rate of 3 Hz applied to the auxiliary trigger inputs. However, each trigger input has 4–5 ps r.m.s. of jitter, which causes a random offset in the acquisition start time. This timing offset effectively adds a linear spectral phase to each spectral slice that is proportional to the start time error. If the triggering error is not taken into account, the slices are combined with incorrect relative phases. Using the overlap between adjacent slices, the start time error of each oscilloscope is estimated and removed with only 100 fs of residual timing error.

Received 23 October 2009; accepted 21 January 2010; published online 28 February 2010

References

1. Takiguchi, K., Okamoto, K., Kominato, T., Takahashi, H. & Shibata, T. Flexible pulse waveform generation using silica-waveguide-based spectrum synthesis circuit. *Electron. Lett.* **40,** 537–538 (2004).
2. Mandai, K., Suzuki, T., Tsuda, H., Kurokawa, T. & Kawanishi, T. Arbitrary optical short pulse generator using a high-resolution arrayed-waveguide grating. *IEEE Topical Meeting on Microwave Photonics* 107–110 (2004).
3. Jiang, Z., Huang, C.-B., Leaird, D. E. & Weiner, A. M. Optical arbitrary waveform processing of more than 100 spectral comb lines. *Nature Photon.* **1,** 463–467 (2007).
4. Scott, R. P. *et al.* Rapid updating of optical arbitrary waveforms via time-domain multiplexing. *Opt. Lett.* **33,** 1068–1070 (2008).
5. Dorrer, C. High-speed measurements for optical telecommunication systems. *IEEE J. Sel. Top. Quantum Electron.* **12,** 843–858 (2006).
6. Li, G. Recent advances in coherent optical communication. *Adv. Opt. Photon.* **1,** 279–307 (2009).
7. Yu, J. & Zhou, X. Multilevel modulations and digital coherent detection. *Opt. Fiber Technol.* **15,** 197–208 (2009).
8. Berezovsky, J., Mikkelsen, M. H., Stoltz, N. G., Coldren, L. A. & Awschalom, D. D. Picosecond coherent optical manipulation of a single electron spin in a quantum dot. *Science* **320,** 349–352 (2008).
9. Solli, D. R., Ropers, C., Koonath, P. & Jalali, B. Optical rogue waves. *Nature* **450,** 1054–1057 (2007).
10. Schikora, S., Wunsche, H. J. & Henneberger, F. All-optical noninvasive chaos control of a semiconductor laser. *Phys. Rev. E* **78,** 025202 (2008).
11. Trebino, R. *Frequency-Resolved Optical Gating: The Measurement of Ultrashort Laser Pulses* (Kluwer Academic, 2000).
12. Dorrer, C. & Joffre, M. Characterization of the spectral phase of ultrashort light pulses. *Comptes Rendus de l'Académie des Sciences, Series IV (Physics-Astrophysics)* **2,** 1415–1426 (2001).
13. O'Shea, P., Kimmel, M., Gu, X. & Trebino, R. Highly simplified device for ultrashort-pulse measurement. *Opt. Lett.* **26,** 932–934 (2001).
14. Panasenko, D. & Fainman, Y. Single-shot sonogram generation for femtosecond laser pulse diagnostics by use of two-photon absorption in a silicon CCD camera. *Opt. Lett.* **27,** 1475–1477 (2002).
15. Fontaine, N. K., Scott, R. P., Heritage, J. P. & Yoo, S. J. B. Near quantum-limited, single-shot coherent arbitrary optical waveform measurements. *Opt. Express* **17,** 12332–12344 (2009).
16. Supradeepa, V. R., Leaird, D. E. & Weiner, A. M. Single shot amplitude and phase characterization of optical arbitrary waveforms. *Opt. Express* **17,** 14434–14443 (2009).
17. Reid, D. T. & Cormack, I. G. Single-shot sonogram: a real-time chirp monitor for ultrafast oscillators. *Opt. Lett.* **27,** 658–660 (2002).
18. Dorrer, C. Single-shot measurement of the electric field of optical waveforms by use of time magnification and heterodyning. *Opt. Lett.* **31,** 540–542 (2006).
19. Bennett, C. V. Ultrafast time scale transformation and recording utilizing parametric temporal imaging. *Digest of the IEEE/LEOS Summer Topical Meetings* 180–181 (IEEE, 2007).
20. Lepetit, L., Chériaux, G. & Joffre, M. Linear techniques of phase measurement by femtosecond spectral interferometry for applications in spectroscopy. *J. Opt. Soc. Am. B* **12,** 2467–2474 (1995).
21. Chu, K. C. *et al.* Direct measurement of the spectral phase of femtosecond pulses. *Opt. Lett.* **20,** 904–906 (1995).
22. Iaconis, C. & Walmsley, I. A. Self-referencing spectral interferometry for measuring ultrashort optical pulses. *IEEE J. Quantum Electron.* **35,** 501–509 (1999).
23. Asghari, M. H., Park, Y. & Azaña, J. Real-time spectral interferometry for single-shot complex-field linear characterization of sub-nanosecond long ultrafast optical signals. *22nd Annual Meeting of the IEEE Photonics Society* Technical Digest (CD) (IEEE, 2009).
24. Kornelis, W. *et al.* Single-shot kilohertz characterization of ultrashort pulses by spectral phase interferometry for direct electric-field reconstruction. *Opt. Lett.* **28,** 281–283 (2003).
25. Bowlan, P. *et al.* Crossed-beam spectral interferometry: a simple, high-spectral-resolution method for completely characterizing complex ultrashort pulses in real time. *Opt. Express* **14,** 11892–11900 (2006).
26. Dorrer, C., Belabas, N., Likforman, J.-P. & Joffre, M. Spectral resolution and sampling issues in Fourier-transform spectral interferometry. *J. Opt. Soc. Am. B* **17,** 1795–1802 (2000).
27. Han, Y. & Jalali, B. Photonic time-stretched analog-to-digital converter: fundamental concepts and practical considerations. *J. Lightwave Technol.* **21,** 3085–3103 (2003).
28. Chou, J., Sefler, G. A., Conway, J., Valley, G. C. & Jalali, B. 4-channel continuous-time 77 GSa/s ADC using photonic bandwidth compression. *2007 IEEE International Topical Meeting on Microwave Photonics* 54–57 (IEEE, 2007).
29. Taylor, M. G. Coherent detection method using DSP for demodulation of signal and subsequent equalization of propagation impairments. *IEEE Photon. Technol. Lett.* **16,** 674–676 (2004).
30. Kazovsky, L., Welter, R., Elrefaie, A. F. & Sessa, W. Wide-linewidth phase diversity homodyne receivers. *J. Lightwave Technol.* **6,** 1527–1536 (1988).
31. Davis, A., Pettitt, M., King, J. & Wright, S. Phase diversity techniques for coherent optical receivers. *J. Lightwave Technol.* **5,** 561–572 (1987).
32. Savory, S. J., Gavioli, G., Killey, R. I. & Bayvel, P. Electronic compensation of chromatic dispersion using a digital coherent receiver. *Opt. Express* **15,** 2120–2126 (2007).
33. Kikuchi, K. Electronic post-compensation for nonlinear phase fluctuations in a 1,000-km 20-Gbit/s optical quadrature phase-shift keying transmission system using the digital coherent receiver. *Opt. Express* **16,** 889–896 (2008).
34. Lyons, R. G. *Understanding Digital Signal Processing* 2nd edn (Prentice Hall PTR, 2004).

35. Velazquez, S. R., Nguyen, T. Q., Broadstone, S. R. & Roberge, J. K. A hybrid filter bank approach to analog-to-digital conversion. *Proceedings of the IEEE-SP International Symposium on Time-Frequency and Time-Scale Analysis* 116–119 (IEEE, 1994).
36. Ding, G., Dehollain, C., Declercq, M. & Azadet, K. Frequency-interleaving technique for high-speed A/D conversion. *Proceedings of the 2003 International Symposium on Circuits and Systems* (*ISCAS '03*) 857–860 (IEEE, 2003).
37. Pupalaikis, P. J. *Digital Bandwidth Interleaving Technical Report* (LeCroy, 2005).
38. Agrawal, G. P. *Lightwave Technology: Components and Devices* (John Wiley & Sons, 2004).
39. Fujiwara, M., Kani, J., Suzuki, H., Araya, K. & Teshima, M. Flattened optical multicarrier generation of 12.5 GHz spaced 256 channels based on sinusoidal amplitude and phase hybrid modulation. *Electron. Lett.* **37,** 967–968 (2001).
40. Sakamoto, T., Kawanishi, T. & Izutsu, M. Asymptotic formalism for ultraflat optical frequency comb generation using a Mach–Zehnder modulator. *Opt. Lett.* **32,** 1515–1517 (2007).
41. Scott, R. P. *et al.* High-fidelity line-by-line optical waveform generation and complete characterization using FROG. *Opt. Express* **15,** 9977–9988 (2007).
42. Fontaine, N. K. *et al.* Compact 10 GHz loopback arrayed-waveguide grating for high-fidelity optical arbitrary waveform generation. *Opt. Lett.* **33,** 1714–1716 (2008).
43. Yuen, H.P. & Chan, V. W. S. Noise in homodyne and heterodyne detection. *Opt. Lett.* **8,** 177–179 (1983).
44. Schumaker, B. L. Noise in homodyne detection. *Opt. Lett.* **9,** 189–191 (1984).
45. Quinlan, F., Ozharar, S., Gee, S. & Delfyett, P. J. Harmonically mode-locked semiconductor-based lasers as high repetition rate ultralow noise pulse train and optical frequency comb sources. *J. Opt. A* **11,** 103001 (2009).
46. Soref, R. The past, present and future of silicon photonics. *IEEE J. Sel. Top. Quantum Electron.* **12,** 1678–1687 (2006).
47. Yoo, S. J. B. Future prospects of silicon photonics in next generation communication and computing systems. *Electron. Lett.* **45,** 584–588 (2009).
48. Doerr, C. R. *et al.* Monolithic silicon coherent receiver. *National Fiber Optic Engineers Conference* OSA Technical Digest (CD) paper PDPB2 (Optical Society of America, 2009).
49. Cheben, P. *et al.* A high-resolution silicon-on-insulator arrayed waveguide grating microspectrometer with sub-micrometer aperture waveguides. *Opt. Express* **15,** 2299–2306 (2007).
50. Sun, H., Wu, K.-T. & Roberts, K. Real-time measurements of a 40 Gb/s coherent system. *Opt. Express* **16,** 873–879 (2008).

Acknowledgements

The authors would like to recognize J. Lowell, E. Ippen, B. Jacobs and E. Parra for their constant encouragement and enlightening discussions and also thank Tektronix for the loan of equipment. This work was supported in part by the Defense Advanced Research Projects Agency (DARPA) and the Space and Naval Warfare Command (SPAWAR) under OAWG contract no. HR0011-05-C-0155.

Author contributions

Data were collected by N.K.F. and R.P.S. and analysed by N.K.F. The experiment was designed by N.K.F. and R.P.S. The OAWM concept was conceived by N.K.F. with contributions from R.P.S., J.P.H. and S.J.B.Y. The OAWM PLC was designed by L.Z. and F.M.S. The manuscript was prepared by N.K.F. and R.P.S. with contributions from J.P.H. and S.J.B.Y. S.J.B.Y. supervised and coordinated all work.

Additional information

The authors declare no competing financial interests. Supplementary information accompanies this paper at www.nature.com/naturephotonics. Reprints and permission information is available online at http://npg.nature.com/reprintsandpermissions/. Correspondence and requests for materials should be addressed to N.K.F.